J|A|C|S COMMUNICATIONS

Published on Web 02/03/2010

In Situ Characterization of the 5d Density of States of Pt Nanoparticles upon Adsorption of CO

Pieter Glatzel,*,† Jagdeep Singh,‡ Kristina O. Kvashnina,† and Jeroen A. van Bokhoven*,‡

European Synchrotron Radiation Facility (ESRF), 6 Rue Jules Horowitz, BP220, 38043 Grenoble Cedex 9, France, and Institute for Chemical and Bioengineering, ETH Zürich, 8093 Zürich, Switzerland

Received September 18, 2009; E-mail: glatzel@esrf.fr; j.a.vanbokhoven@chem.ethz.ch

Nanoparticles of noble metals on different supports are able to catalyze chemical reactions. This property is used extensively in many everyday applications, such as automotive catalytic converters,[1] and on a large industrial scale for production of raw materials and fine chemicals.[2] Changes in catalytic performance are driven by changes in the electronic structure of the valence shell.[3] The availability of valence orbitals to form chemical bonds and thus to participate in the catalytic reaction depends on their electron occupation and energy.

Experimental studies of the electronic structure of catalytically active nanoparticles under working conditions are challenging. Few experimental techniques are compatible with the required high-temperature gas environment and the low metal concentration of supported nanoparticles. The pioneering work by Ertl and co-workers[4] demonstrated the power of valence-band photoemission spectroscopy (UPS) to study the adsorption of molecules on metal surfaces. A hard X-ray photon-in/photon-out technique has lower energy resolution[5] but is far less restrictive than UPS with respect to the sample environment and is furthermore truly element-selective. Resonant inelastic X-ray scattering is a technique that combines the element selectivity of inner-shell spectroscopies with charge-neutral (i.e., nonionizing) excitations within the valence shell as typically done in UV−vis spectroscopy.[6,7] It thus becomes possible to probe the electronic structure around the Fermi level at the catalytically active site. In this communication, we report a study of the unoccupied and occupied d density of states (DOS) upon adsorption of CO on supported Pt nanoparticles.

We used in situ high-energy-resolution fluorescence-detected (HERFD) X-ray absorption spectroscopy (XAS)[8] and resonant inelastic X-ray scattering (RIXS). In these techniques, the energies of incident and emitted (scattered) X-rays are analyzed by means of Bragg reflections from perfect crystals. Scheme 1 illustrates the energy levels that are involved. An incident photon of energy Ω excites a Pt 2p electron into the 5d level. The excited electronic states form the X-ray absorption spectrum. These states decay with a lifetime τ upon emission of a photon with energy ω. The energy deposited in the sample is the energy transfer, $\Omega - \omega$, which, if it is sufficiently small, corresponds to a charge-neutral excitation within the 5d shell. The experiments yield a two-dimensional intensity distribution that is plotted versus the incident (absorption) energy Ω and the final state energy $\Omega - \omega$. The lifetime τ of the 2p core hole broadens the spectrum along the incident energy direction but not along the energy transfer axis.[5]

The RIXS planes of Pt nanoparticles after reduction and hydrogen removal and after adsorption of CO are shown in Figure 1. In the present study, we worked at the Pt L_3 ($2p_{3/2}$) edge, which has a large absorption cross section. The horizontal line of intensity at zero energy transfer is denoted the elastic peak. It arises either from absorption and decay paths according to Scheme 1 with equal incident and emitted energies or from non-element-selective Thomson scattering from the sample.[7] The intensity of the latter contribution is not a function of the Pt absorption and thus does not follow the absorption cross section. The feature serves as an absolute energy calibration in the experiment because it indicates the case where no energy is deposited in the sample (i.e., where the energy transfer $\Omega - \omega$ is zero).

Scheme 1. Energy Diagram for RIXS at the Pt L Edge

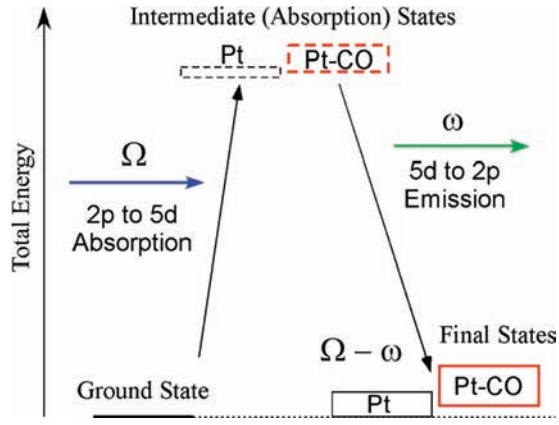

The RIXS planes show intensity at a few electron volts of energy transfer. This transfer arises from valence-band ("optical") excitations. We note that optically forbidden transitions in UV−vis spectroscopy may become allowed in RIXS because of the two-photon nature of the process. In the case of Pt nanoparticles, the elastic peak and the valence-band excitations merge together, indicating a metallic electronic structure. This means that the Fermi level lies within a partially filled band. After adsorption of CO on the Pt nanoparticles, an increase in intensity above 4 eV of energy transfer is observed, and a broad energy distribution develops. A gap opens up between the elastic peak at zero energy transfer and the lowest unoccupied electronic states that can be reached in the RIXS process.

Electronic structure calculations were performed using the multiple scattering formalism as implemented in the FEFF8.4 program.[9] This code calculates the density of states and projects it onto the spherical angular moments for each atom that is included in the structure. The Pt d DOS was inserted into the following equation to calculate the theoretical RIXS planes:[7,10]

$$F(\Omega,\omega) = \int_{\varepsilon} \mathrm{d}\varepsilon \frac{\rho_{\mathrm{d}}(\varepsilon)\rho'_{\mathrm{d}}(\varepsilon + \Omega - \omega)}{(\varepsilon - \omega)^2 + \frac{\Gamma_{\mathrm{n}}^2}{4}} \qquad (1)$$

† European Synchrotron Radiation Facility.
‡ ETH Zürich.

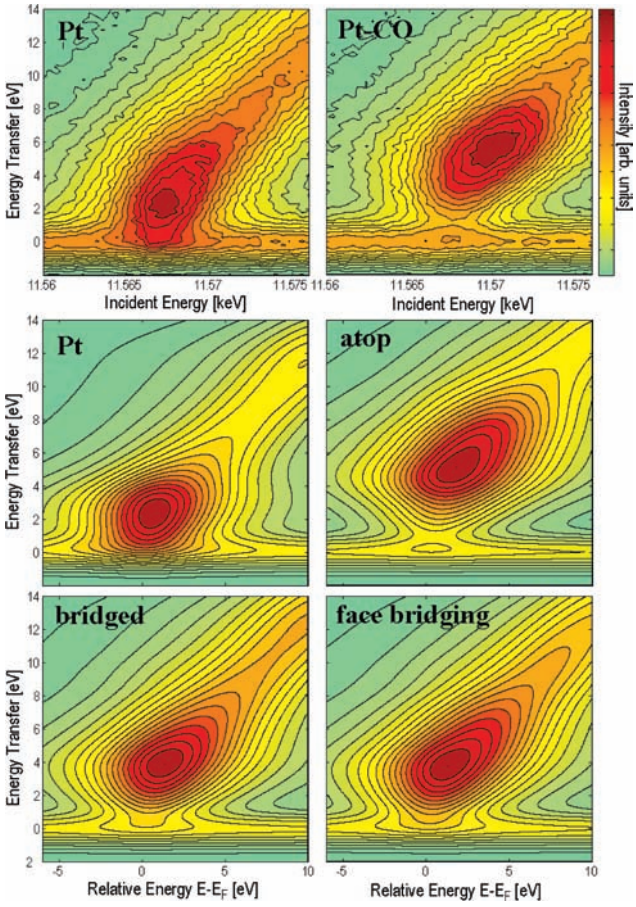

Figure 1. (top) $2p_{3/2}$ RIXS planes of supported Pt nanoparticles: (left) metallic and (right) with CO adsorbed. (bottom) Calculated RIXS planes for a bare Pt_6 cluster and the cluster with CO coordinated at three different sites.

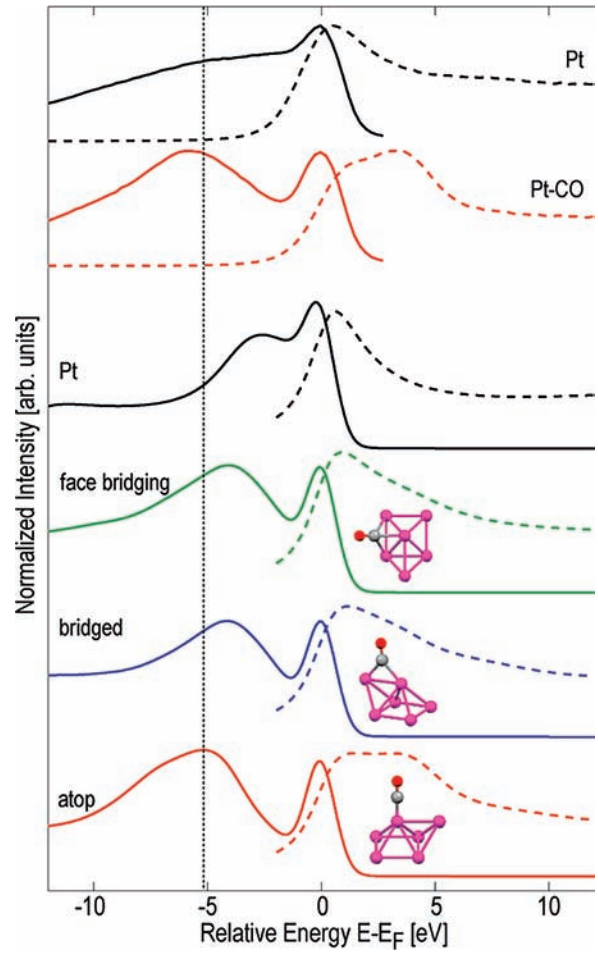

Figure 2. (top) Experimental HERFD L_3 XAS (dashed) and RIXS (solid) data. (bottom) Calculated HERFD XAS and RIXS data for Pt_6 and Pt_6 with CO coordinated at three different sites. The dotted vertical line is a guide to the eye.

where ρ and ρ' are the densities of occupied and unoccupied Pt d states, respectively, and Γ_n denotes the lifetime broadening of the $2p_{3/2}$ core hole, which is 5.4 eV. The approximations in this approach for calculating the RIXS spectral shape have been discussed elsewhere.[7,10] Briefly, we use the ground-state electronic structure and neglect all interactions due to the photoexcitation process. No strict theoretical argument exists to justify this approximation, and its validity is evaluated by comparison between experiment and theory.

We calculated the RIXS planes for a bare Pt_6 cluster and the cluster with CO adsorbed at three different sites (Figure 1). An elastic peak due to Thomson scattering was added to the RIXS planes to facilitate comparison with experiment. The RIXS plane for the Pt_6 cluster nicely reproduces the metallic character that we described for the experimental results. Adsorption of CO gives rise to a shift in the maximum RIXS intensity to higher energy transfer. While the shift is approximately equal when CO is adsorbed in bridged or face-bridging sites, it is observably more pronounced for CO adsorbed to a single Pt atom in an atop configuration.

Figure 2 combines the RIXS data with the experimental HERFD absorption scans. The RIXS spectral intensity in Figure 1 was summed along the incident energy (i.e., the horizontal direction) to give line plots with the elastic peak at zero energy. The energy transfer in Figure 1 was multiplied by -1 for comparison with the absorption spectra. The energy of the elastically scattered peak corresponds to the energy of the Fermi level. The elastic peak was not subtracted from the data because it was not possible to distinguish between intensity that must be attributed to Pt and that due to non-element-specific Thomson scattering.

The atop configuration provides the best agreement with the experimental absorption and RIXS data. A pronounced high-energy shoulder in the absorption spectrum has already been reported by Safonova et al.[11] The calculations for the bridged and face-bridging configurations cannot reproduce the pronounced shift of the RIXS peak maximum to lower relative energies.

The structure of the Pt_6 cluster was proposed by Janin et al.[12] and has been shown to be a good representation of Pt nanoparticles in spectroscopic calculations.[13] More accurate modeling of the systems may be achieved by considering a larger cluster, changing the shape of the particle, adding more CO to the particle, and including a support. The broad distribution of the RIXS spectral shape in comparison with the Pt_6 calculations indicates that several cluster species are present. This also holds for the structures of the CO-absorbed particles. The relative spectral changes, however, are independent of these considerations, and the main experimental results are captured by the simple model.

Equation 1 directly relates the electron density to the RIXS spectra. We compare the calculated orbital angular momentum-projected densities of states in Figure 3. The Pt 5d band is almost filled, and the Fermi level is close to the top of the 5d band. With

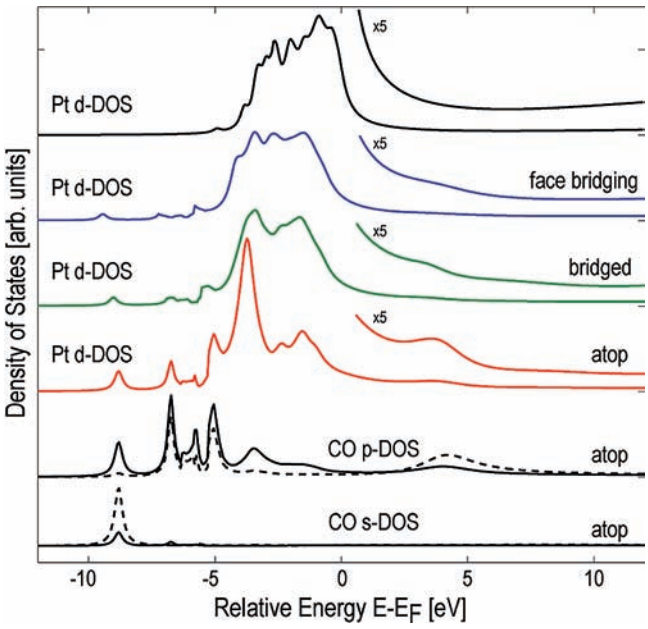

Figure 3. Calculated orbital angular momentum-projected densities of states. The d DOS for Pt_6 and Pt coordinated to CO in three configurations of a Pt_6CO cluster and the p and s DOS for C (dashed) and O (solid) are shown.

CO adsorbed on Pt, bonding, nonbonding, and antibonding orbitals are formed. The antibonding orbitals above the Fermi level are unoccupied and split the white line of the absorption spectrum that probes the empty Pt d DOS.[11] They show predominantly carbon p DOS. Occupied orbitals that are strongly hybridized between CO and Pt appear in the calculated DOS between −3 and −9 eV relative energy. At the lowest energy, the CO p and s DOS hybridize, forming a strong bonding orbital in which the p and s DOS are mainly localized on oxygen and carbon, respectively. The electron density distribution in the π orbitals has been described in terms of an allylic molecular orbital diagram.[14]

In total, the Pt d DOS in the bare particle at energies just below the Fermi level is transferred to lower energies, where Pt and CO orbitals strongly hybridize.[15] The d states that arise from adsorption of CO on Pt are most populated for the atop configuration, confirming that this model forms the most stable Pt−CO bond. Even though the RIXS spectra cannot resolve the DOS fine structure, the stronger bond between CO and the Pt cluster is reflected by the shift of the RIXS maximum to lower relative energy. Similarly, the antibonding states in the atop configuration at ∼4 eV give rise to the pronounced shoulder in the absorption spectrum.

The bonding states are barely visible in the X-ray emission spectrum as a low-energy tail, but they are clearly observed in non-element-selective UPS.[16] The two techniques have different spectral sensitivities. Nonresonant photoemission also includes the ligand s and p DOS, which emphasizes the bonding orbitals, while RIXS at the Pt L_3 edge selectively probes the Pt d DOS, which has less density in the bonded states.

The experiments show that the center of mass of the 5d band moves to lower energy. The experimentally observed trends are well-reproduced in the calculated spectra. Comparison with the DOS of the adsorbed CO shows that this change of spectral weight arises from orbitals that are hybridized between Pt d and ligand p and s orbitals. Thus, the valence electrons populate deeper binding energies because of the bond that is formed with CO. This mechanism is most pronounced in the atop configuration.

The data shows how the electronic structure of Pt nanoparticles changes with adsorption of CO. Consequently, the electronic, magnetic, and catalytic properties are altered. Moving the d band to lower energies decreases the tendency of the particles to form bonds with reactants, thus affecting the catalytic activity.[2] CO adsorption thus poisons the surface of a catalyst, by both blocking sites and altering the intrinsic catalytic activity of the catalyst.

Acknowledgment. We thank the ESRF support groups and the ID26 staff for their invaluable help, Dr. Jeffrey T. Miller for providing the samples, Dr. Olga Safonova for help with the calculations, Dr. Janine Grattage for correcting the manuscript, and the Swiss National Science Foundation for financial support.

Supporting Information Available: Materials and Methods. This material is available free of charge via the Internet at http://pubs.acs.org.

References

(1) Farrauto, R. J.; Heck, R. M. *Catal. Today* **1999**, *51*, 351.
(2) *Handbook of Heterogeneous Catalysis*, 2nd ed.; Ertl, G., Knözinger, H., Schüth, F., Weitkamp, J., Eds.; Wiley-VCH: Weinheim, Germany, 2008; Vol. 8.
(3) Hammer, B.; Nørskov, J. K. *Nature* **1995**, *376*, 238. Hammer, B.; Nørskov, J. K. *Surf. Sci.* **1995**, *343*, 211. Bligaard, T.; Nørskov, J. K.; Dahl, S.; Matthiesen, J.; Christensen, C. H.; Sehested, J. *J. Catal.* **2004**, *224*, 206.
(4) Conrad, H.; Ertl, G.; Küppers, J.; Latta, E. E. *Faraday Discuss.* **1974**, *58*, 116. Paal, Z.; Schlogl, R.; Ertl, G. *J. Chem. Soc., Faraday Trans.* **1992**, *88*, 1179. Bao, X.; Wild, U.; Muhler, M.; Pettinger, B.; Schlögl, R.; Ertl, G. *Surf. Sci.* **1999**, *425*, 224. Huang, W. X.; Bao, X. H.; Rotermund, H. H.; Ertl, G. *J. Phys. Chem. B* **2002**, *106*, 5645.
(5) Glatzel, P.; Bergmann, U. *Coord. Chem. Rev.* **2005**, *249*, 65.
(6) de Groot, F. Kotani, A. *Core Level Spectroscopy of Solids*; CRC Press: Boca Raton, FL, 2008; Vol. 6.
(7) Kotani, A.; Shin, S. *Rev. Mod. Phys.* **2001**, *73*, 203.
(8) Hämäläinen, K.; Siddons, D. P.; Hastings, J. B.; Berman, L. E. *Phys. Rev. Lett.* **1991**, *67*, 2850. van Bokhoven, J. A.; Louis, C.; Miller, J. T.; Tromp, M.; Safonova, O. V.; Glatzel, P. *Angew. Chem., Int. Ed.* **2006**, *45*, 4651.
(9) Ankudinov, A. L.; Ravel, B.; Rehr, J. J.; Conradson, S. D. *Phys. Rev. B* **1998**, *58*, 7565. Rehr, J. J.; Albers, R. C. *Rev. Mod. Phys.* **2000**, *72*, 621. Ankudinov, A. L.; Rehr, J. J.; Low, J.; Bare, S. R. *Phys. Rev. Lett.* **2001**, *86*, 1642.
(10) Jimenez-Mier, J.; van Ek, J.; Ederer, D. L.; Callcott, T. A.; Jia, J. J.; Carlisle, J.; Terminello, L.; Asfaw, A.; Perera, R. C. *Phys. Rev. B* **1999**, *59*, 2649.
(11) Safonova, O. V.; Tromp, M.; van Bokhoven, J. A.; de Groot, F. M. F.; Evans, J.; Glatzel, P. *J. Phys. Chem. B* **2006**, *110*, 16162.
(12) Janin, E.; von Schenck, H.; Gothelid, M.; Karlsson, U. O.; Svensson, M. *Phys. Rev. B* **2000**, *61*, 13144.
(13) Lewis, E. A.; Segre, C. U.; Smotkin, E. S. *Electrochim. Acta* **2009**, *54*, 7181.
(14) Nilsson, A.; Pettersson, L. G. M. *Surf. Sci. Rep.* **2004**, *55*, 49.
(15) Blyholder, G. *J. Phys. Chem.* **1964**, *68*, 2772. Chen, L.; Chen, B.; Zhou, C.; Wu, J.; Forrey, R. C.; Cheng, H. *J. Phys. Chem. C* **2008**, *112*, 13937. Valero, M. C.; Raybaud, P.; Sautet, P. *J. Catal.* **2007**, *247*, 339.
(16) Alnot, M.; Cassuto, A.; Ducros, R.; Ehrhardt, J. J.; Weber, B. *Surf. Sci.* **1982**, *114*, L48.

JA907760P